Recent Results from PHENIX

Ron Belmont[1,*] for the PHENIX Collaboration

[1]University of North Carolina at Greensboro

Abstract. We present results from the heavy-ion physics program of the PHENIX experiment at RHIC. These results include jet substructure, open heavy flavor, charmonium, strangeness, electromagnetic probes, femtoscopy, and flow.

1 Introduction

Since ending operations in the summer of 2016, the PHENIX Collaboration has continued to data analysis of the wide variety of high-quality data collected in the last few years of operations. These proceedings represent a subset of recent results, as presented at the Strangeness in Quark Matter conference held in Busan, Korea in June of 2022. These results include measurements of jet substructure, open heavy flavor, charmonium, strangeness, electromagnetic probes, femtoscopy, and flow.

2 Jet Substructure

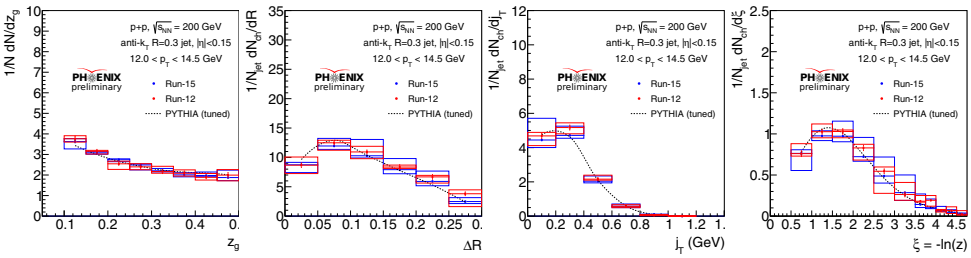

Figure 1. New preliminary results on jet substructure measurements in p+p collisions at $\sqrt{s}$ = 200 GeV, from left to right: jet splitting function, radial profile, transverse fragmentation, longitudinal fragmentation.

Shown in Figure 1 is a variety of new preliminary results on jet substructure measurements in p+p collisions at $\sqrt{s}$ = 200 GeV. A single jet p_T bin, 12.0 GeV/c < p_T < 14.5 GeV/c, is shown; additional p_T bins have been measured and will be presented in a forthcoming publication. The jets are reconstructed using the anti-k_T algorithm with a jet radius of $R = 0.3$. From left to right, shown are: the jet splitting function dN/dz_g as a function of z_g; the radial profile $dN_{\rm ch}/dR$ as a function of ΔR; the transverse fragmentation $dN_{\rm ch}/dj_T$ as

*e-mail: rjbelmon@uncg.edu

a function of j_T; the longitudinal fragmentation $dN_{\rm ch}/d\xi$ as a function of ξ. These measurements provide important detailed information about the substructure of jets in p+p collisions and also provide the baseline for future measurements in p+Au.

3 Open Heavy Flavor Results

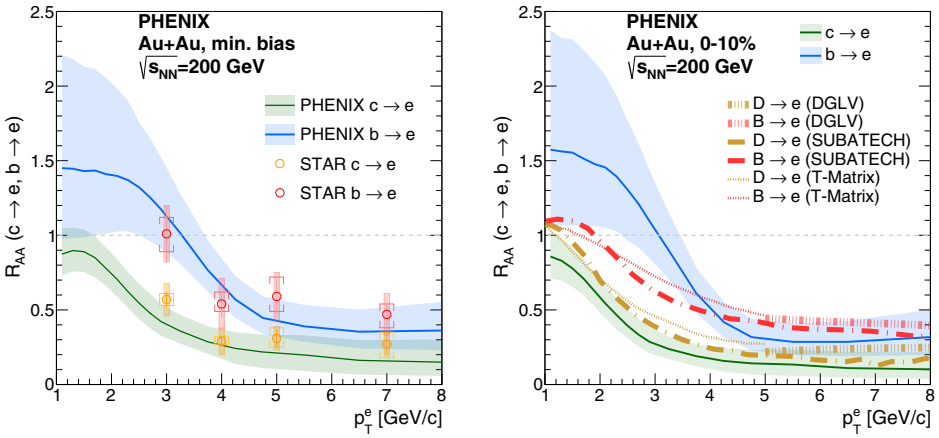

Figure 2. R_{AA} of $c \rightarrow e$ and $b \rightarrow e$ for minimum bias Au+Au collisions at $\sqrt{s_{NN}}$ = 200 GeV [1] with comparisons to STAR measurements (left panel) and model calculations (right panel).

Some open heavy flavor results are shown in Figure 2, R_{AA} of $c \rightarrow e$ and $b \rightarrow e$ for minimum bias Au+Au collisions at $\sqrt{s_{NN}}$ = 200 GeV [1]. The left panel shows a comparison to STAR measurements and demonstrates good agreement between the experiments. The right panel shows a comparison to various theoretical models, demonstrating good agreement for charm at all p_T as well as good agreement for bottom at higher p_T.

4 Charmonium

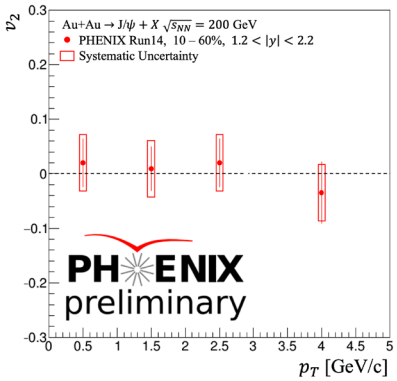

Figure 3. Anisotropy coefficient v_2 of J/ψ for $1.2 < |\eta| < 2.2$ in Au+Au collisions at $\sqrt{s_{NN}}$ = 200 GeV.

Shown in Figure 3 is the v_2 of J/ψ for $1.2 < |\eta| < 2.2$ in Au+Au collisions at $\sqrt{s_{NN}} = 200$ GeV. The v_2 of J/ψ at forward/backward rapidity at RHIC energies is consistent with zero. This is contrast with the non-zero v_2 found at mid-rapidity at RHIC energies, as well as the non-zero v_2 found at both mid- and forward/backward rapidity at LHC energies. This may indicate the absence of regeneration at forward/backward rapidity at RHIC energies.

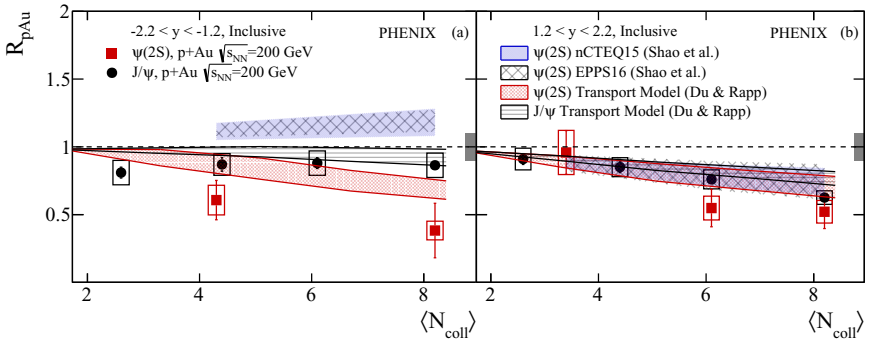

Figure 4. nuclear modification factor R_{AB} of J/ψ and $\psi(2S)$ for $1.2 < |\eta| < 2.2$ in p+Au collisions at $\sqrt{s_{NN}} = 200$ GeV [2].

Figure 4 shows the nuclear modification factor R_{AB} of J/ψ and $\psi(2S)$ at forward and backward rapidity ($1.2 < |\eta| < 2.2$) in p+Au collisions at $\sqrt{s_{NN}} = 200$ GeV [2].

The J/ψ modification is consistent with initial state effects alone at forward and backward rapidity. Likewise is true for the $\psi(2S)$ at forward rapidity, but contrariwise, the $\psi(2S)$ modification indicates presence of final state effects at backward rapidity. The final state effects could be the presence of co-movers, or perhaps an indication of the presence of the quark-gluon plasma (QGP).

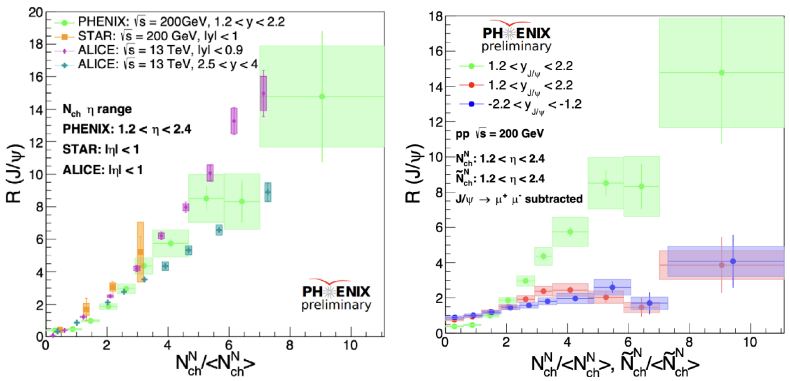

Figure 5. Relative yield of J/ψ in p+p collisions at $\sqrt{s_{NN}} = 200$ GeV. In the left panel, the multiplicity is determined in the same kinematic region as the J/ψ is reconstructed. In the right panel, the multiplicity is determined in a different kinematic region, and compared to the result when the multiplicity is reconstructed in the same region but when the J/ψ contribution to the multiplicity is subtracted off.

Figure 5 shows the relative yield of J/ψ in p+p collisions at $\sqrt{s_{NN}} = 200$ GeV. Relative yield of J/ψ in p+p collisions at $\sqrt{s_{NN}} = 200$ GeV. In the left panel, the multiplicity is determined in the same kinematic region as the J/ψ is reconstructed. Both forward and backward

rapidity selections are compared. In the right panel, the multiplicity is determined in a different kinematic region, and compared to the result when the multiplicity is reconstructed in the same region but when the J/ψ contribution to the multiplicity is subtracted off.

The dramatic reduction in J/ψ enhancement when either selecting multiplicity in a different kinematic region, or when adjusting the multiplicity to account for the J/ψ itself, may have considerable implications for the rule of multi-parton interactions in J/ψ production.

5 Strangeness

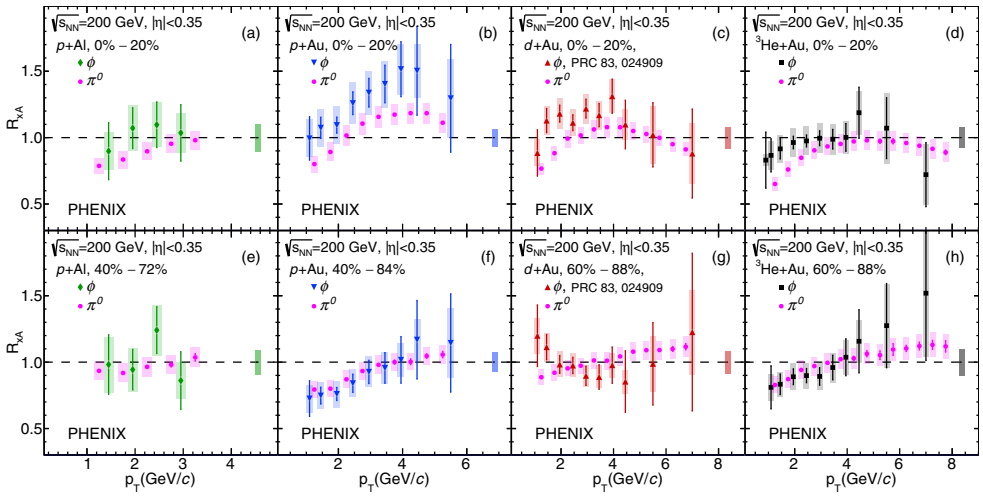

Figure 6. Nuclear modification factor R_{AB} of ϕ mesons in p+Al, p+Au, d+Au, and ^{3}He+Au collisions at $\sqrt{s_{NN}}$ = 200 GeV [3]. The upper row shows the most central collisions and the lower row shows the most peripheral collisions.

Figure 6 shows nuclear modification factor R_{AB} of ϕ mesons in p+Al, p+Au, d+Au, and ^{3}He+Au collisions at $\sqrt{s_{NN}}$ = 200 GeV [3]. The ϕ is mostly consistent with the π^0 in nearly all cases, perhaps suggesting a lack of apparent strangeness enhancement in small systems. However, allowing for the relatively large experimental uncertainties, there is some slight indication of enhancement in central collisions for p+Au, d+Au, and ^{3}He+Au collisions.

6 Electromagnetic Probes

Figure 7 shows nuclear modification factor R_{AB} of π^0 mesons in p+Al, p+Au, d+Au, and ^{3}He+Au collisions at $\sqrt{s_{NN}}$ = 200 GeV [4]. The centrality selection is 0–10% for all four. Seen at intermediate p_T is the usual Cronin enhancement. This enhancement is smaller when the target nucleus is lighter, viz. the R_{AB} of π^0 is smaller in p+Al than it is in p+Au. Additionally, the enhancement is also smaller when the projectile is heavier, as seen in the decreasing trend of the enhancement from p+Au to d+Au and then to ^{3}He+Au.

Shown in Figure 8 is the R_{AB} of π^0 determined using the standard MC Glauber $N_{\rm coll}$ (left panel), the R_{AB} of direct photons determined using the standard MC Glauber $N_{\rm coll}$ (center panel), and the R_{AB} of π^0 determined using experimentally determined $N_{\rm coll}$ (right panel).

It is known direct photons are not modified by nuclear matter, with a mean free path approximately 50 times larger than the nuclear size. Because of this, the R_{AB} of direct photons

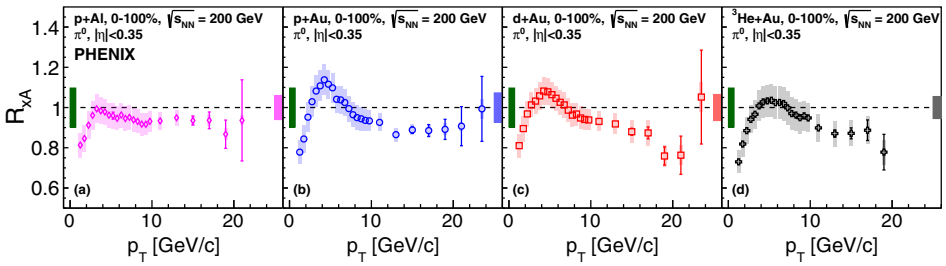

Figure 7. Nuclear modification factor R_{AB} of π^0 in p+Al, p+Au, d+Au, and ^{3}He+Au collisions at $\sqrt{s_{NN}}$ = 200 GeV [4]. Minimum-bias 0–100% is shown for all four collision species.

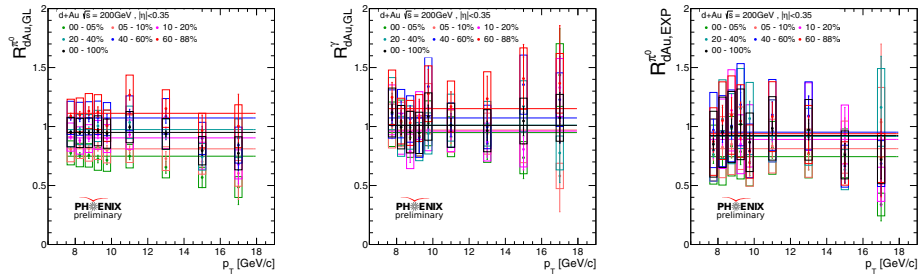

Figure 8. Nuclear modification factor R_{AB} of π^0 (left, right) and direct photon (center). in d+Au collisions at $\sqrt{s_{NN}}$ = 200 GeV. Various centralities are shown. For the left and center panels, the standard MC Glauber determination of $N_{\rm coll}$ is used. On the right, experimentally determined $N_{\rm coll}$ is used instead.

should be exactly unity. The apparent deviation from unity is an indication of event selection bias. The experimentally determined $N_{\rm coll}$ adjusts for this bias by enforcing the direct photon R_{AB} to be exactly unity. When using these new values of $N_{\rm coll}$ to determine the R_{AB} of π^0, the apparent enhancement seen in the left panel is removed in the right panel. This addresses the long-standing mystery of the peripheral enhancement as not being due to some novel physics effect but rather an event selection bias. Contrariwise, the slight suppression of the R_{AB} of π^0 persists when correcting for this bias. The origin of this effect is not yet understood, but could be due to the EMC effect in the nuclear PDFs and/or an indication of suppression caused by the QGP.

7 Flow

The azimuthal triangular anisotropy v_3 of charged hadrons in p+Au, d+Au, and ^{3}He+Au collisions at $\sqrt{s_{NN}}$ = 200 GeV [5] is shown in Figure 9.

The agreement between the 3×2PC method and the event plane method indicates the robustness of the measurement against sensitive experimental effects like the detector alignment and beam optics.

Although results are not shown here due to length restrictions, we want to call your attention to another recent PHENIX publication on a systematic study of the centrality and system size dependence of v_2 in p+p, p+Au, d+Au, and ^{3}He+Au collisions at $\sqrt{s_{NN}}$ = 200 GeV [6]

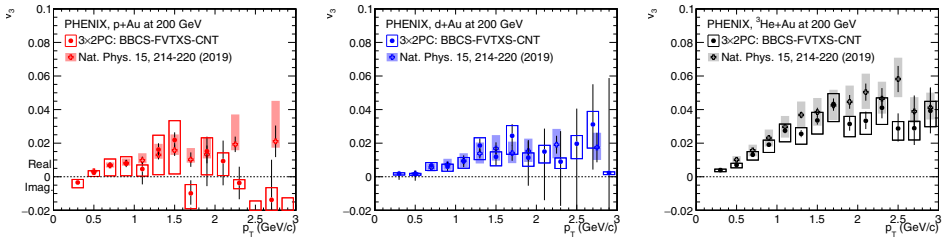

Figure 9. Azimuthal triangular anisotropy v_3 of charged hadrons in p+Au, d+Au, and ^{3}He+Au collisions at $\sqrt{s_{NN}}$ = 200 GeV. The most central 0–5% is shown for all three collision species. Data from Ref. [5]

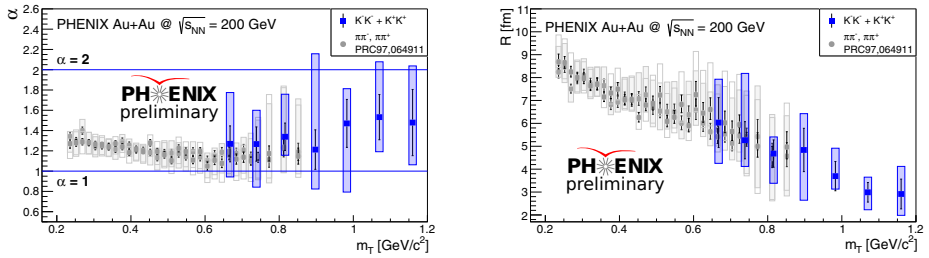

Figure 10. HBT with kaons. Source shape parameter α vs pair m_T is shown in the left panel. Radius parameter R vs pair m_T is shown in the right panel.

8 Femtoscopy

Figure 10 shows the source shape parameter α (left panel) and the radius parameter R (right panel) as a function of the pair m_T. By using a Lévy function, the source shape can be better understood in comparison to a typical Gaussian function. When $\alpha = 1$ the source is equivalent to a Cauchy distribution, and to a Gaussian when $\alpha = 2$. The measurement indicates a source shape somewhere in between but closer to a Cauchy distribution. The results using $\pi^{\pm}$ and $K^{\pm}$ show similar trends, with the charged kaon results continuing to higher pair m_T due to the larger mass of the individual particles.

9 Summary

PHENIX continues to produce high-quality physics results on a variety of topics, including but not limited to jet substructure, open heavy flavor, charmonium, strangeness, electromagnetic probes, femtoscopy, and flow as shown in these proceedings. Further results and publications are forthcoming, and we are looking forward to sharing them at the next SQM.

References

[1] PHENIX Collaboration, arXiv:2203.17058, submitted to Phys. Rev. C (2022)
[2] PHENIX Collaboration, Phys. Rev. C **105, 064912 (2022)**
[3] PHENIX Collaboration, Phys. Rev. C 106, 014908 (2022)
[4] PHENIX Collaboration, Phys. Rev. C 105, 064902 (2022)
[5] PHENIX Collaboration, Phys. Rev. C 105, 024901 (2022)
[6] PHENIX Collaboration, arXiv:2203.09894, submitted to Phys. Rev. C (2022)